Applied Surface Science 652 (2024) 159370

Contents lists available at ScienceDirect

Applied Surface Science

journal homepage: www.elsevier.com/locate/apsusc

Full Length Article

In-situ spectral reflectance investigation of hetero-epitaxially grown β-Ga_2O_3 thin films on c-plane Al_2O_3 via MOVPE process

Ta-Shun Chou [a,*], Saud Bin Anooz [a], Raimund Grüneberg [a], Jana Rehm [a], Arub Akhtar [a], Deshabrato Mukherjee [b,c], Peter Petrik [b,d], Andreas Popp [a]

[a] Leibniz-Institut für Kristallzüchtung (IKZ), Max-Born-Str. 2, 12489 Berlin, Germany
[b] Institute for Technical Physics and Materials Science, Centre for Energy Research, Konkoly Thege Miklos Str. 29-33, 1121 Budapest, Hungary
[c] Doctoral School of Materials Sciences and Technologies, Óbuda University, Budapest, Hungary
[d] Faculty of Science and Technology, University of Debrecen, P.O. Box 400, Debrecen 4002, Hungary

ARTICLE INFO

Keywords:
A1. Surfaces
A3. Metalorganic vapor phase epitaxy
B1. Gallium compounds

ABSTRACT

Metalorganic vapor-phase epitaxy of β-Ga_2O_3/c-plane Al_2O_3 heterostructures was monitored *in-situ* by spectral reflectance in different wavelengths. The reflectance spectrum was analysed as a function of the growth time and the incident wavelength to estimate the growth rate and the refractive index at the growth temperatures. The obtained values are validated by *ex-situ* methods such as secondary ion mass spectrum measurement and spectroscopic ellipsometry. A theoretical simulation of the reflectance spectrum was carried out by combining a transfer matrix method with a multilayer model, and a good agreement with the experimental results is presented.

1. Introduction

In recent years, there has been an increasing focus on β-Ga_2O_3 for different heterostructure electronic device applications, such as high breakdown voltage devices [1–3], Schottky diodes [4], photodetectors [5–8], and gas sensing devices [9,10]. The increasing interest in β-Ga_2O_3 is mainly due to its excellent properties with an ultrawide bandgap of about 4.8 eV [11] and its consequent high electric breakdown field of up to 8 MV/cm [12]. Many techniques have been investigated for the heteroepitaxy process of β-Ga_2O_3 films to fulfill the requirements of device fabrication on different substrates, especially on c-plane Al_2O_3, including pulsed laser deposition (PLD) [8,13], molecular beam epitaxy (MBE) [14,15], halide vapor phase epitaxy (HVPE) [16,17], and metalorganic vapor phase epitaxy (MOVPE) [18–24].

Among the techniques mentioned above, the MOVPE technique offers many advantages for device fabrication, including homogeneous deposition over device topography and the capability for large-scale production. The growth evolution of heteroepitaxial β-Ga_2O_3 thin films using MOVPE is believed to be linked to structural imperfections and the functional properties of the final layers. Traditional characterization methods such as transmission electron microscopy (TEM), scanning electron microscopy (SEM), and secondary ion mass spectroscopy (SIMS) have been used to evaluate the structural qualities, interfacial properties, and thickness of β-Ga_2O_3 films grown by MOVPE. However, these methods are time-consuming, destructive, and ex-situ, making them impractical for production purposes.

Therefore, there is a high demand for a non-destructive, in-situ monitoring tool. Reflectance-based methods, such as reflection high-energy electron diffraction (RHEED) [25,26], have been widely used in various deposition techniques for in-situ monitoring. However, RHEED is typically limited to specific growth environments, such as low temperatures or vacuum conditions [27], making it suitable only for certain tools like molecular beam epitaxy (MBE) and pulsed laser deposition (PLD) but not for MOVPE. To our present knowledge, there have been no *in-situ* observations of the heteroepitaxial β-Ga_2O_3/c-plane Al_2O_3 growth process in the MOVPE system due to the lack of available refractive index at high temperatures. To fill this gap, we demonstrated using reflectance spectroscopy (RS) to *in-situ* monitor the thin film growth rate and the refractive index at high temperatures with validation by high-temperature ellipsometry measurement. Simulation methods like effective medium approximation (EMA) and transfer matrix method (TMM) are used to interpret observed reflected signals and correlate them with film properties and spectroscopic ellipsometry (SE) measurements [28,29]. This addresses limitations in commercial

* Corresponding author.
E-mail address: ta-shun.chou@ikz-berlin.de (T.-S. Chou).

https://doi.org/10.1016/j.apsusc.2024.159370
Received 29 June 2023; Received in revised form 7 December 2023; Accepted 8 January 2024
Available online 10 January 2024

software, which may lack specific material parameters and flexibility for simultaneous estimation of growth rate and surface roughness based on user-defined layer structures. The results obtained in this work are an important step towards the high-quality β-Ga_2O_3-based optoelectronic devices and the growth process control of β-Ga_2O_3-related alloys, β-$(Al_xGa_{1-x})_2O_3$/β-Ga_2O_3 [30–32].

2. Methods

2.1. Experimental setup

The MOVPE system was utilized to grow Si-doped β-Ga_2O_3 thin films consisting of a vertical shower-head low-pressure reactor (Structured Materials Industries, Inc. -USA). Triethylgallium (TEGa) was used as the metalorganic precursor for Ga, and Tetraethylorthosilicate (TEOS) was used as the metalorganic precursor for the n-type doping by Si, while O_2 (5 N) was used as the oxidant, and high purity Ar (5 N) acts as the carrier gas. Commercial c-plane Al_2O_3 of dimensions size 10 × 10 × 0.5 mm^3 was prepared by CrysTec GmbH. β-Ga_2O_3 thin film growth was performed at a constant growth temperature of 800 °C to ensure the formation of β-phase, and the chamber pressure was kept at 25 mbar. The Ar flow rate through the chamber was constant at 235 × 10^{-3} mol/min. Thin films were grown using TEGa molar flow rates of range between 1.9 × 10^{-5} mol/min and 5.5 × 10^{-5} mol/min, and the oxygen molar flow rates varied between 7 × 10^{-3} mol/min and 2.2 × 10^{-2} mol/min. The TEOS molar flow rates range from 4 × 10^{-11} mol/min to 3 × 10^{-8} mol/min. During the thin film deposition, *in-situ* reflectance monitoring was performed by using a Laytec EpiNet system (EpiNet 2017, Laytec. -Germany), acquiring reflectance signals at 405 nm, 633 nm, and 950 nm with the LED light sources through a window normal to the substrate embedded on the top of the MOVPE chamber [33]. The light source module is switched on and off several times per revolution (200 Hz modulation). One revolution is sufficient to acquire all measurement data of the samples that sit within the same radius of the susceptor. The thin-film thickness and the Si concentration were determined by the secondary ion mass spectrometry (SIMS) performed by RTG Mikroanalyse GmbH Berlin. The films were structurally characterized by high-resolution x-ray diffraction (HR-XRD) using a Bruker D8 instrument behind a pre-collimating parabolic Göbel mirror, and an asymmetric Ge 220 double crystal monochromator was utilized to select the Cu Kα1 line at λ = 1.540 56 Å and to collimate the incident x-ray beam to about 36 arcsec. The surface morphology of the grown β-Ga_2O_3 films was investigated by atomic force microscopy (AFM) (Bruker Dimension Icon, USA). The room-temperature and temperature-dependent optical properties of the β-Ga_2O_3 thin film were determined by spectroscopic ellipsometry (SE) on a Woollam M-2000DI rotating compensator ellipsometer in the spectral range of 0.73 to 6.5 eV at an angle of incidence equal to 60°. Temperature-dependent SE measurements were carried out from room temperature (RT) and finally ramped up to 800 ℃, and it should be noted that the stability of the sample was checked by comparing the spectra measured before and after the SE measurement, showing that the sample did not deteriorate during the procedure.

2.2. A multilayer stack simulation

The Effective Medium Approximation (EMA) is a widely utilized method for modeling the optical characteristics and ellipsometry parameters of thin films. It employs the effective dielectric function to estimate the surface roughness and employs two parameters to describe the roughness: the volume fraction and the thickness of the rough surface layer. In the EMA approach, the surface roughness layer is typically assumed to consist of a combination of bulk material and air. The void volume is assumed to remain constant at 50 %, while the thickness of the surface roughness layer is adjusted as an unknown parameter through the fitting.

Optical constants like the dielectric function ε and the complex refractive index N are needed to perform the EMA simulation. The dielectric function can be expressed as a function of the complex refractive index as $\varepsilon = N^2$ following the Maxwell equations, the complex refractive index N is defined as $N \equiv n + ik$ with n as the refractive index and k as the extinction coefficient. The surface roughness layer is generally assumed to be homogeneous with an effective dielectric function, ε_{eff}. The effective dielectric function of the surface roughness layer can be calculated based on a simplified microscopic model, with the polarization of components represented by point dipoles [34] in the following form (Eq. (1)):

$$f\frac{\boldsymbol{\varepsilon_n} - \boldsymbol{\varepsilon_{eff}}}{\boldsymbol{\varepsilon_n} + \boldsymbol{\varepsilon_{eff}}} + (1-f)\frac{\boldsymbol{\varepsilon_v} - \boldsymbol{\varepsilon_{eff}}}{\boldsymbol{\varepsilon_v} + \boldsymbol{\varepsilon_{eff}}} = 0 \quad (1)$$

where f and ε_n represent the volume fraction and dielectric function of the measured sample, respectively; ε_v is the dielectric function of void spaces.

With the suggested optical structure from the EMA, the Transfer Matrix Method (TMM) is widely used as a mathematical approach to investigating wave reflection and transmission in one-dimensional structures, mostly on thin film. Considering the case of the heteroepitaxy process, a simplified four-layer structure, as shown in Figure SI 1, is proposed to represent the grown film. n_1, n_2 and n_3 are the real refractive index of the vacuum, the grown film (β-Ga_2O_3), and the substrate (c-plane Al_2O_3), respectively, while n_{eff} is the refractive index of the effective layer, d is the thickness of the β-Ga_2O_3 epilayer, and d_{eff} is the thickness of the effective layer. The light propagates in each layer according to the plane of incidence under an incident angle θ with respect to the reflection plane. Following Ref. [35], by projecting the electromagnetic wave vectors on the reflection plane with the boundary conditions at the interfaces, the Fresnel reflection coefficients r_s and r_p from layer 1 to layer 2 can be obtained as Eq. (2) and Eq. (3):

$$r_s = \frac{n_1\cos\theta_1 - n_2\cos\theta_2}{n_1\cos\theta_1 + n_2\cos\theta_2} \quad (2)$$

$$r_p = \frac{n_2\cos\theta_1 - n_1\cos\theta_2}{n_2\cos\theta_1 + n_1\cos\theta_2} \quad (3)$$

The Fresnel reflection coefficients involving more layers and interfaces can be determined with the same formulation. Together with the TMM, the total reflectivity of the film can be, therefore, expressed in the recurrence matrix form between the layers depicted in Figure SI 1, and a detailed deduction to calculate the total reflectivity can be found in Ref. [35,36].

3. Results and discussion

At optimal growth conditions, β-Ga_2O_3 grows with the $(\bar{2}01)$ orientation parallel to (0001) Al_2O_3 plane [37,38]. Fig. 1 illustrates the 2θ-ω HR-XRD scan of the β-Ga_2O_3 film on c-plane Al_2O_3. In the 2θ range from 10° to 80°, only $(\bar{2}01)$, $(\bar{4}01)$ and $(\bar{6}01)$ Bragg peaks of the monoclinic gallium oxide phase can be detected. The Inset of Fig. 1 shows the XRD rocking curve of the $(\bar{2}01)$ diffraction peak of the β-Ga_2O_3 thin film. The full width at half maximum (FWHM) of the rocking curve is measured as 1.30°, indicating no significant dislocation densities. As a comparison, the reported FWHMs of β-Ga_2O_3 thin films grown on c-plane sapphire substrates are 1.5° (MOCVD, $(\bar{2}01)$ diffraction peak) [37] and 1.49° (LPCVD, $(\bar{2}01)$ diffraction peak)[39]. Fig. 2 shows *in-situ* collected reflectance spectra with wavelengths of 405 nm, 633 nm, and 950 nm from a ~ 1000 nm heteroepitaxial grown β-Ga_2O_3 film on c-plane Al_2O_3. Fabry-Perot (FP) oscillations appear in reflectance transients as the film growth starts due to differences in the refractive index of c-plane Al_2O_3 ($n_{Al_2O_3}$ = 1.77 as the nominal value [40] at room temperature) and β-Ga_2O_3 ($n_{Ga_2O_3}$ = 1.95 as the nominal value [41] at room temperature). Amplitudes of interference oscillation after a certain growth time are gradually getting smaller. Finally, no oscillation can be observed when

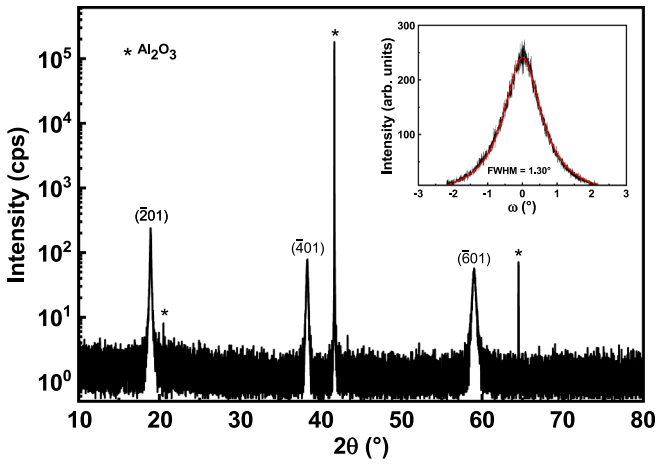

Fig. 1. 2θ-ω scans for the β-Ga_2O_3 thin film grown on the on-axis c-plane sapphire. Inset XRD rocking curve of $(\bar{2}01)$ reflection of β-Ga_2O_3 thin film.

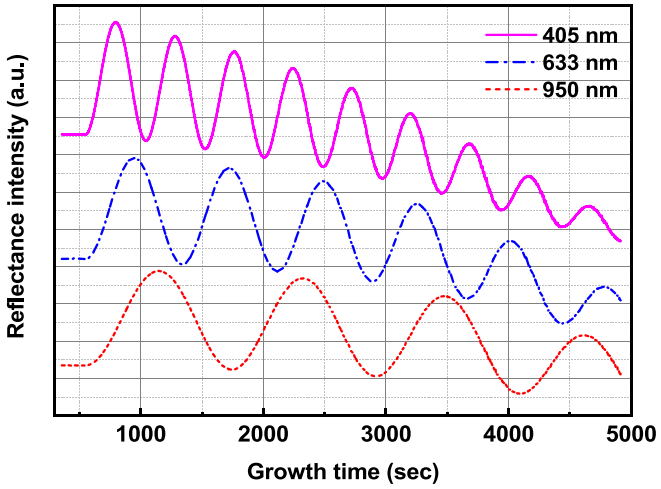

Fig. 2. *In-situ* reflectance transients recorded during the film growth at different wavelengths of 405 nm, 633 nm, and 950 nm.

the film is over a certain thickness, which is attributed to the increasing light scattering from the roughening surface (see Fig. 3) due to three-dimensional (3D) island growth caused by large lattice mismatch (~10.60 %) between Al_2O_3 and β-Ga_2O_3 [42].

Besides, it can also be observed from Fig. 2 that the reflectance reduction is more pronounced at a smaller wavelength, which can be described qualitatively as [43] (Eq. (4)):

$$\boldsymbol{R(t)}\ \boldsymbol{R_0 e^{-(4\pi\sigma/\lambda)^2}} \tag{4}$$

where R_0 is the initial reflectance value, and σ is the root-mean-square (RMS) roughness of the sample surface. Following Eq. (4), when considering a decrease in surface roughness, a smaller incident wavelength exhibits a higher sensitivity by experiencing a relatively significant reduction compared to longer wavelengths. This phenomenon arises because the reflectance near the normal angle relies on both the surface roughness and the diffuse reflectance, with the latter being more prominent at smaller wavelengths and negligible at longer wavelengths [43].

From the peak-to-peak (or valley-to-valley) distance of the oscillation at the selected wavelength, $\tau(\lambda)$ (sec), the growth rate can be calculated by applying the FP equation for the interference oscillations (Eq. (5)):

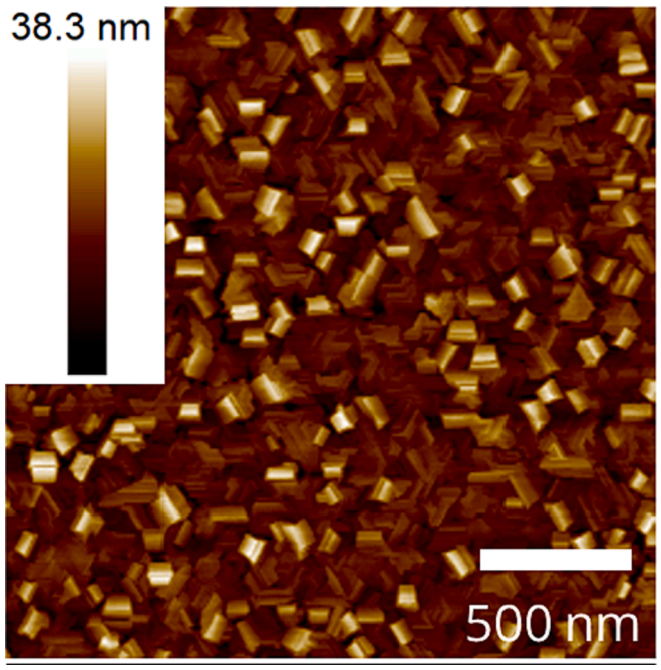

Fig. 3. AFM images of a β-Ga_2O_3 thin film grown on c-plane Al_2O_3 with a thickness of around 150 nm.

$$\text{Growth rate (nm/sec)} = \frac{\lambda}{2n(\lambda, T)\tau(\lambda)} \tag{5}$$

where λ is the wavelength of the incident light (nm), $n(\lambda, T)$ is the refractive index of the grown film at the incident wavelength, λ, and at growth temperature, T. To estimate the growth rate from FP oscillation, one should consider the thermo-optic effect while determining the refractive index since the reflectance transient is recorded at 800 °C. However, there was no measured value of the refractive index for $(\bar{2}\,01)$ β-Ga_2O_3 at high temperatures up to 800 °C. Therefore, to determine the refractive index of the β-Ga_2O_3 film at high temperature (800 °C), temperature-dependent SE measurements were performed from room temperature up to 800 °C. To evaluate the refractive index and bandgap energy, we used a model to fit the SE parameters, Ψ and Δ, which consists of a four-component stack composed of substrate/film/ surface roughness/air, as shown in Figure SI 1. The optical properties of the surface roughness layer are analyzed by a Bruggeman effective medium approximation [44] consisting of a 50 % bulk film/50 % void mixture.

The experimentally measured ellipsometry parameters, ψ and Δ, which are related to the optical and structural properties of the sample, are defined as (Eq. (6)):

$$\rho = \frac{R_p}{R_s} = \tan(\Psi)e^{i\Delta} \tag{6}$$

where R_p and R_s are the complex reflection coefficients of the light-polarized parallel (p) and perpendicular (s) to the plane of incidence, respectively. While β-Ga_2O_3 films heteroepitaxial grown on c-plane Al_2O_3 substrates contain threefold in-plane rotational domains[45], SE data were analyzed by assuming an isotropic material.

Since the films under investigation are optically transparent in the 0.73 – 4.3 eV spectral range, here the dispersion of the refractive index can be evaluated by the Sellmeier dispersion equation (first approximation, Eq. (7)):

$$n^2(\lambda, T) = 1 + \frac{B\lambda^2}{\lambda^2 - \lambda_0^2} \tag{7}$$

where B is a fitting parameter proportional to the density of effective

electron states, and λ_0 is the wavelength of the Sellmeier oscillator. The values of B and λ_0 at room temperature and 800 ℃ are listed in Table 1. The extinction coefficient k is considered to be zero since the absorption of the β-Ga_2O_3 film in the visible region can be neglected[46]. Based on the Sellmeier dispersion relation, we determined the refractive index of β-Ga_2O_3 film in the transparent region (Fig. 4). It is obvious that the refractive index continuously increases with decreasing the wavelength. Nearly the same dispersion behavior is observed for β-Ga_2O_3 films and bulk [45,46].

The evaluated n at 405 nm, 633 nm, and 905 nm of β-Ga_2O_3 film as a function of temperature is presented in Fig. 5. The refractive index at the three wavelengths reveals an increase with increasing temperature, and this behavior is attributed to electron–phonon interaction that is enhanced with increasing temperature [47].

Refractive indices for all three wavelengths at RT and 800 °C have been tabulated in Table 2. The value of n, especially at 633 nm (~1.93), is larger than the one reported by other authors [41,48]. As the higher n indicates more dense films without pores, this means that the MOVPE technique results in denser Ga_2O_3 layers. This can also explain the higher dielectric constant as compared to films deposited by other techniques.

It has been reported by Bhaumik [41] et al. that β-Ga_2O_3 (in (1 0 0) and (0 1 0) planes) has a positive thermo-optic coefficient around 10^{-5}/ K in the temperature range of 30 °C to 175 °C. Fig. 5 shows the measured refractive indices as a function of temperature from room temperature to 800 °C at different wavelengths, and a slope of ~ 10^{-5}/ K can be observed, matching the reported values in the literature [41,48]. Table 3 summarizes the thermo-optic coefficients at different wavelengths from Fig. 5.

In Fig. 6a, the heteroepitaxial growth of a 300 nm Si-doped β-Ga_2O_3 film is monitored at different wavelengths. Using the refractive index at 800 °C and 405 nm from Table 2, the reflectivity response at 405 nm of the heteroepitaxial structure (Fig. 6a) has been fitted by a theoretical simulation model essentially based on the TMM simulation package in Python [36] and the four-layer stack structure (Figure SI 1).

In the following simulation, n_1, n_2 and n_3 are the real refractive index of the air, the film (β-Ga_2O_3), and the substrate (c-plane Al_2O_3), respectively. We have used the obtained refractive indices of β-Ga_2O_3 (Table 2) and the refractive indices of c-plane Al_2O_3 (at 800 ℃) [40,49]. The refractive index of the effective layer, n_{eff}, is calculated by fitting the reflectance spectrum at 405 nm. The simulation results given by the model are presented by the green line in Fig. 7. The two parameters which characterize the effective layer are the effective refractive index, n_{eff}, and the effective thickness, d_{eff}, respectively [50]. d_{eff} is obtained from the best fitting of the experimentally collected reflectance signals as a function of time from Fig. 7.

The simulation result of the *in-situ* reflectance gives the β-Ga_2O_3 layer thickness of ~ 300 nm, and an effective layer thickness of about 25 nm can be determined, matching the cross-sectioned scanning electron microscopy (SEM) image and the SIMS profile of the film shown in Fig. 6b and Fig. 6c, respectively. On the other hand, ellipsometry is an optical method that accurately determines the optical constants of surfaces or the thickness and optical constants of superficial films on solid substrates [51,52]. Therefore, on the same sample, SE measurements have been performed, and the best-fitting adjustment gives a layer thickness of 299 nm and an effective thickness surface roughness of about 12 nm. The film thickness is in good agreement with the film thickness determined by SIMS and the *in-situ* reflectance. However, the noticeable

Table 1
A summary of the Sellmeier coefficients equation (Eq. (7)) at room temperature and 800℃.

Coefficient	Room temp.	800 °C
B	2.59 ± 0.02	2.63 ± 0.02
λ_0 (nm)	136 ± 3	149 ± 3

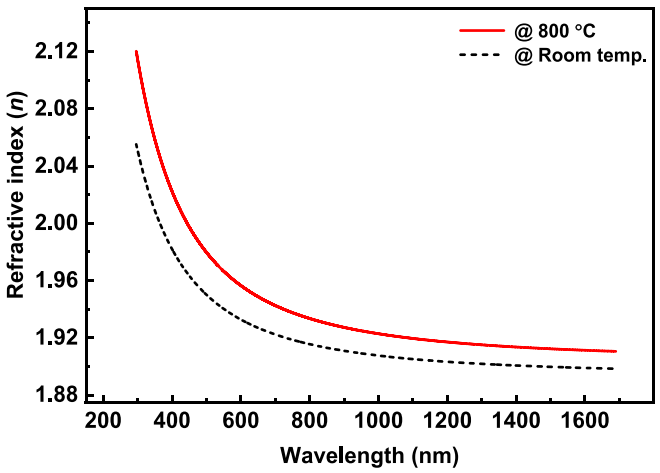

Fig. 4. The refractive index obtained by using a Sellmeier dispersion relation from experimentally measured Ψ and Δ spectra of β-Ga_2O_3 on c-plane Al_2O_3 at room temperature and 800 °C.

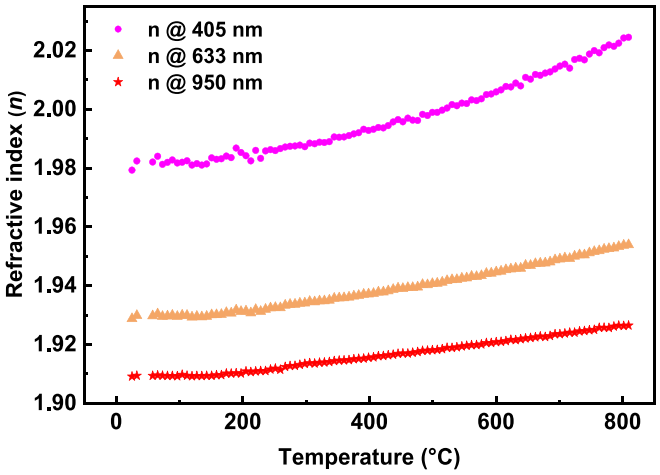

Fig. 5. The temperature-dependent refractive index of β-Ga_2O_3 on c-plane Al_2O_3 ranges from RT to 800 °C at the wavelengths of 405 nm, 633 nm, and 950 nm.

Table 2
The refractive index of β-Ga_2O_3 on c-plane Al_2O_3 at room temperature and 800 °C.

Wavelength (nm)	Refractive index	
	Room temp.	800 °C
405	1.98 ± 0.01	2.02 ± 0.01
633	1.93 ± 0.01	1.95 ± 0.01
950	1.90 ± 0.01	1.93 ± 0.01

Table 3
The thermo-optic coefficient of β-Ga_2O_3 on c-plane Al_2O_3 at different wavelengths.

Wavelength (nm)	Thermo-optic coefficient (1/K)
405	5.8×10^{-5}
633	3.2×10^{-5}
950	2.2×10^{-5}

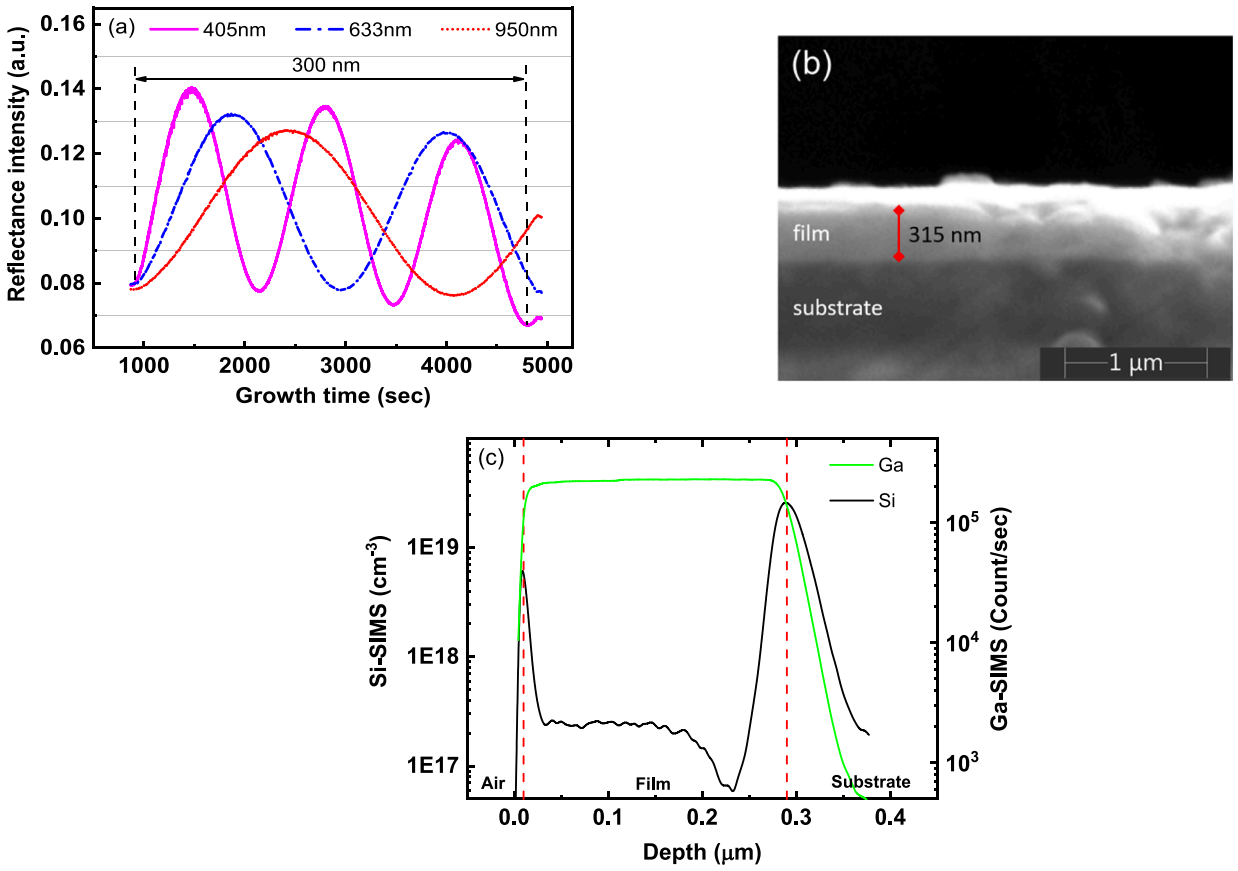

Fig. 6. (a) Reflectance transients (curves) recorded during sample growth at different wavelengths of 405 nm, 633 nm, and 950 nm, and the evolution of the spectra during the growth. (b) A SEM image (cross-section view) of the film from Fig. 6a. (c) The depth profile determined by the SIMS measurement via the intentionally doped Si concentration and the Ga intensity in the film from Fig. 6a.

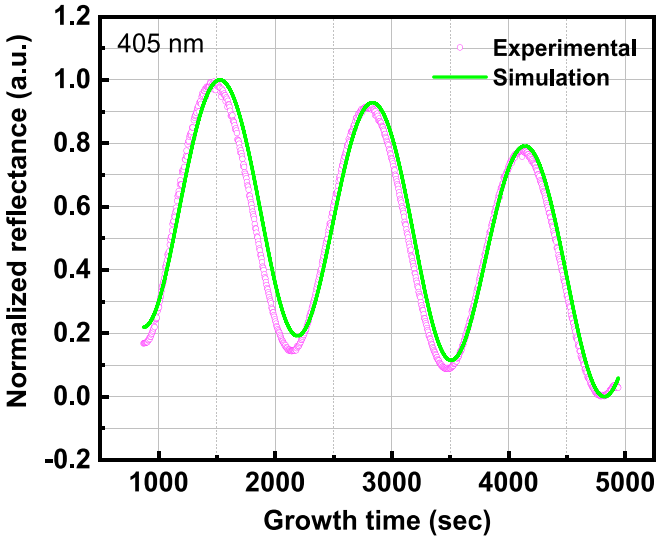

Fig. 7. The best fit of the normalized reflectance (from Fig. 6a) obtained from reflectance spectroscopy using the effective layer/β-Ga_2O_3/c-plane Al_2O_3 substrate system at an incident wavelength of 405 nm.

difference in the effective layer thickness (25 nm from the reflectance spectrum and 12 nm from SE) can be attributed to variations in spot size between reflectance spectroscopy and spectroscopic ellipsometry and local roughness fluctuations on the film surface. Moreover, it is anticipated that the total film thickness may deviate by approximately 5 % due to temperature-induced expansion (using a temperature expansion coefficient of approximately $\sim 1 \times 10^{-5}$/ K [42,53]. To check the validity and reproducibility of the model, several β-Ga_2O_3 films were grown on c-plane Al_2O_3 substrate at different deposition times. The film thickness values obtained from *in-situ* reflectance fitted by TMM and *ex-situ* SE measurements are comparable and presented in Fig. 8.. A good match between the simulation results (triangles) and the experimental measurement (circles) is clearly evident.

4. Conclusions

This work investigated the heteroepitaxial growth of β-Ga_2O_3 thin film on c-plane Al_2O_3 using a multiwavelength (405 nm, 633 nm, and 950 nm) *in-situ* monitoring system as well as *ex-situ* spectroscopic ellipsometry. Room temperature and high-temperature (800 °C) refractive index of β-Ga_2O_3 on c-plane Al_2O_3 were determined. The thermo-optic coefficient from room temperature to 800 °C at different wavelengths was reported. The EMA model and the TMM simulation are combined to estimate the β-Ga_2O_3 thin film thickness and surface roughness using the measured high-temperature refractive index and were compared with the *ex-situ* spectroscopic ellipsometry values. A good agreement between the simulation approach and the experimental results is established.

CRediT authorship contribution statement

Ta-Shun Chou: Writing – original draft, Methodology, Investigation, Formal analysis, Data curation. **Saud Bin Anooz:** Writing – original draft, Methodology, Investigation, Formal analysis, Data curation. **Raimund Grüneberg:** Methodology, Data curation. **Jana Rehm:**

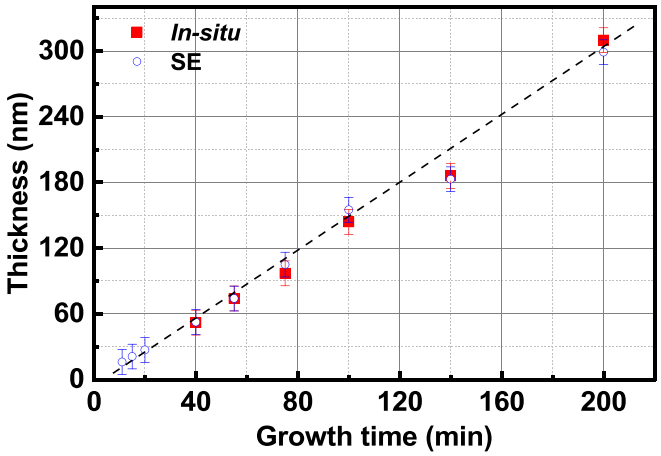

Fig. 8. A comparison between the thickness values obtained from measured values using SE (circles) and the fitted values derived from the in-situ reflectance spectrum (triangles).

Methodology, Data curation. **Arub Ahktar:** Data curation. **Deshabrato Mukherjee:** Methodology, Data curation. **Peter Petrik:** Data curation, Resources, Supervision, Writing – review & editing. **Andreas Popp:** Investigation, Project administration, Resources, Supervision, Writing – review & editing.

Declaration of competing interest

The authors declare that they have no known competing financial interests or personal relationships that could have appeared to influence the work reported in this paper.

Data availability

Data will be made available on request.

Acknowledgment

The authors thank Dr. Martin Schmidbauer for reading the manuscript and Sabine Bergmann for the support of SEM characterization. This work was performed in the framework of GraFOx, a Leibniz ScienceCampus. The work was funded by the BMBF under grant number 16ES1084K, the European Community (Europäische Fonds für regionale Entwicklung- EFRE) under grant number 1.8/15, and by the Deutsche Forschungsgemeinschaft under project funding reference number PO-2659/1-2. Support from OTKA grant Nr. 131515 is also greatly acknowledged.

Author contributions

Ta-Shun Chou and Saud Bin Anooz contributed equally to this work.

References

[1] K. Tetzner, O. Hilt, A. Popp, S. Bin Anooz, J. Würfl, Challenges to overcome breakdown limitations in lateral β-Ga2O3 MOSFET devices, Microelectron. Reliab. 114 (2020) 113951, https://doi.org/10.1016/j.microrel.2020.113951.
[2] Y. Lü, X. Song, Z. He, Y. Wang, X. Tan, S. Liang, C. Wei, X. Zhou, Z. Feng, Source-field-plated Ga_2O_3 MOSFET with a breakdown voltage of 550 v, J. Semicond. 40 (2019) 012803, https://doi.org/10.1088/1674-4926/40/1/012803.
[3] T.-S. Chou, P. Seyidov, S. Bin Anooz, R. Grüneberg, T. Thi Thuy Vi, K. Irmscher, M. Albrecht, Z. Galazka, J. Schwarzkopf, A. Popp, Fast homoepitaxial growth of (100) β-Ga_2O_3 thin films via MOVPE process, AIP Adv. 11 (2021) 115323. 10.1063/5.0069243.
[4] M.H. Wong, K. Sasaki, A. Kuramata, S. Yamakoshi, M. Higashiwaki, Electron channel mobility in silicon-doped Ga_2O_3 MOSFETs with a resistive buffer layer, Jpn. J. Appl. Phys. 55 (2016) 1202B9, https://doi.org/10.7567/JJAP.55.1202B9.
[5] X.Z. Liu, P. Guo, T. Sheng, L.X. Qian, W.L. Zhang, Y.R. Li, β-Ga_2O_3 thin films on sapphire pre-seeded by homo-self-templated buffer layer for solar-blind UV photodetector, Opt. Mater. (amst) 51 (2016) 203–207, https://doi.org/10.1016/j.optmat.2015.11.023.
[6] S. Müller, L. Thyen, D. Splith, A. Reinhardt, H. Von Wenckstern, M. Grundmann, High-quality Schottky barrier diodes on β-gallium oxide thin films on glass substrate, ECS J. Solid State Sci. Technol. 8 (2019) Q3126–Q3132, https://doi.org/10.1149/2.0241907jss.
[7] B.R. Tak, S. Kumar, A.K. Kapoor, D. Wang, X. Li, H. Sun, R. Singh, Recent advances in the growth of gallium oxide thin films employing various growth techniques—a review, J. Phys. D Appl. Phys. 54 (2021) 453002, https://doi.org/10.1088/1361-6463/ac1af2.
[8] Y. Xu, Z. An, L. Zhang, Q. Feng, J. Zhang, C. Zhang, Y. Hao, Solar blind deep ultraviolet β-Ga_2O_3 photodetectors grown on sapphire by the Mist-CVD method, Opt. Mater. Express 8 (2018) 2941, https://doi.org/10.1364/ome.8.002941.
[9] S. Manandhar, A.K. Battu, A. Devaraj, V. Shutthanandan, S. Thevuthasan, C. V. Ramana, Rapid response high temperature oxygen sensor based on titanium doped gallium oxide, Sci. Rep. 10 (2020) 178, https://doi.org/10.1038/s41598-019-54136-8.
[10] M. Bartic, C.I. Baban, H. Suzuki, M. Ogita, M. Isai, β-Gallium oxide as oxygen gas sensors at a high temperature, J. Am. Ceram. Soc. 90 (2007) 2879–2884, https://doi.org/10.1111/j.1551-2916.2007.01842.x.
[11] V.M. Bermudez, The structure of low-index surfaces of β-Ga_2O_3, Chem. Phys. 323 (2006) 193–203, https://doi.org/10.1016/j.chemphys.2005.08.051.
[12] H. Zhou, J. Zhang, C. Zhang, Q. Feng, S. Zhao, P. Ma, Y. Hao, A review of the most recent progresses of state-of-art gallium oxide power devices, J. Semicond. 40 (2019) 011803, https://doi.org/10.1088/1674-4926/40/1/011803.
[13] F.B. Zhang, K. Saito, T. Tanaka, M. Nishio, Q.X. Guo, Structural and optical properties of Ga_2O_3 films on sapphire substrates by pulsed laser deposition, J. Cryst. Growth 387 (2014) 96–100, https://doi.org/10.1016/j.jcrysgro.2013.11.022.
[14] E.G. Víllora, K. Shimamura, K. Kitamura, K. Aoki, Rf-plasma-assisted molecular-beam epitaxy of β-Ga_2O_3, Appl. Phys. Lett. 88 (2006) 031105, https://doi.org/10.1063/1.2164407.
[15] S. Ghose, M.S. Rahman, J.S. Rojas-Ramirez, M. Caro, R. Droopad, A. Arias, N. Nedev, Structural and optical properties of β-Ga_2O_3 thin films grown by plasma-assisted molecular beam epitaxy, J. Vac. Sci. Technol., B: Nanotechnol. Microelectron.: Mater., Process., Meas., Phenom. 34 (2016) 02L109, https://doi.org/10.1116/1.4942045.
[16] G. Pozina, C.W. Hsu, N. Abrikossova, M.A. Kaliteevski, C. Hemmingsson, Development of β-Ga_2O_3 layers growth on sapphire substrates employing modeling of precursors ratio in halide vapor phase epitaxy reactor, Sci. Rep. 10 (2020) 22261, https://doi.org/10.1038/s41598-020-79154-9.
[17] V.I. Nikolaev, A.I. Pechnikov, S.I. Stepanov, I.P. Nikitina, A.N. Smirnov, A. V. Chikiryaka, S.S. Sharofidinov, V.E. Bougrov, A.E. Romanov, Epitaxial growth of (2^{-} 01) β-Ga2O3 on (0001) sapphire substrates by halide vapour phase epitaxy, Mater. Sci. Semicond. Process. 47 (2016) 16–19, https://doi.org/10.1016/j.mssp.2016.02.008.
[18] Y. Yao, S. Okur, L.A.M. Lyle, G.S. Tompa, T. Salagaj, N. Sbrockey, R.F. Davis, L. M. Porter, Growth and characterization of α-, β-, and ϵ-phases of Ga_2O_3 using MOCVD and HVPE techniques, Mater. Res. Lett. 6 (2018) 268–275, https://doi.org/10.1080/21663831.2018.1443978.
[19] Y. Lv, J. Ma, W. Mi, C. Luan, Z. Zhu, H. Xiao, Characterization of β-Ga2O3 thin films on sapphire (0001) using metal-organic chemical vapor deposition technique, Vacuum 86 (2012) 1850–1854, https://doi.org/10.1016/j.vacuum.2012.04.019.
[20] D. Gogova, M. Schmidbauer, A. Kwasniewski, Homo- and heteroepitaxial growth of Sn-doped β-Ga_2O_3 layers by MOVPE, CrstEngComm 17 (2015) 6744–6752, https://doi.org/10.1039/c5ce01106j.
[21] D. Gogova, G. Wagner, M. Baldini, M. Schmidbauer, K. Irmscher, R. Schewski, Z. Galazka, M. Albrecht, R. Fornari, Structural properties of Si-doped β-Ga_2O_3 layers grown by MOVPE, J. Cryst. Growth 401 (2014) 665–669, https://doi.org/10.1016/j.jcrysgro.2013.11.056.
[22] Y. Ma, W. Tang, T. Chen, L. Zhang, T. He, X. Zhou, X. Wei, X. Deng, H. Fu, K. Xu, X. Zhang, B. Zhang, Effect of off-axis substrate angles on β-Ga_2O_3 thin films and solar-blind ultraviolet photodetectors grown on sapphire by MOCVD, Mater. Sci. Semicond. Process. 131 (2021) 105856, https://doi.org/10.1016/j.mssp.2021.105856.
[23] T.-S. Chou, P. Seyidov, S. Bin Anooz, R. Grüneberg, M. Pietsch, J. Rehm, T.T. V. Tran, K. Tetzner, Z. Galazka, M. Albrecht, K. Irmscher, A. Fiedler, A. Popp, Suppression of particle formation by gas-phase pre-reactions in (100) MOVPE-grown β-Ga2O3 films for vertical device application, Appl. Phys. Lett. 122 (2023) 052102.
[24] T.-S. Chou, P. Seyidov, S. Bin Anooz, R. Grüneberg, J. Rehm, T.T.V. Tran, A. Fiedler, Z. Galazka, M. Albrecht, A. Popp, High-mobility 4 μm MOVPE-grown (100) β-Ga2O3 thin film by parasitic particles suppression, Jpn. J. Appl. Phys. 62 (2023) SF1004.
[25] J. Schörmann, S. Potthast, D.J. As, K. Lischka, In situ growth regime characterization of cubic GaN using reflection high energy electron diffraction, Appl. Phys. Lett. 90 (2007) 041918, https://doi.org/10.1063/1.2432293.
[26] S. Fernández-Garrido, G. Koblmüller, E. Calleja, J.S. Speck, In situ GaN decomposition analysis by quadrupole mass spectrometry and reflection high-energy electron diffraction, J. Appl. Phys. 104 (2008) 033541, https://doi.org/10.1063/1.2968442.
[27] J.H. Neave, P.J. Dobson, B.A. Joyce, J. Zhang, Reflection high-energy electron diffraction oscillations from vicinal surfaces - A new approach to surface diffusion

measurements, Appl. Phys. Lett. 47 (1985) 100–102, https://doi.org/10.1063/1.96281.
[28] I. Massoudi, A. Rebey, Analysis of in situ thin films epitaxy by reflectance spectroscopy: Effect of growth parameters, Superlattice. Microst. 131 (2019) 66–85, https://doi.org/10.1016/j.spmi.2019.05.026.
[29] I. Massoudi, M.M. Habchi, A. Rebey, B. El Jani, Study of surface roughness using spectral reflectance measurements recorded during the MOVPE of InAs/GaAs heterostructures, Phys. E. 44 (2012) 1282–1287, https://doi.org/10.1016/j.physe.2012.02.002.
[30] A.F.M.A.U. Bhuiyan, Z. Feng, L. Meng, A. Fiedler, H.L. Huang, A.T. Neal, E. Steinbrunner, S. Mou, J. Hwang, S. Rajan, H. Zhao, Si doping in MOCVD grown (010) β-(AlxGa1-x)2O3 thin films, J. Appl. Phys. 131 (2022) 145301, https://doi.org/10.1063/5.0084062.
[31] A.F.M. Anhar Uddin Bhuiyan, Z. Feng, J.M. Johnson, H.L. Huang, J. Hwang, H. Zhao, MOCVD Epitaxy of Ultrawide Bandgap β-$(Al_xGa_{1-x})_2O_3$ with High-Al Composition on (100) β-Ga_2O_3 Substrates, Cryst. Growth Des. 20 (2020) 6722–6730. 10.1021/acs.cgd.0c00864.
[32] J. Rehm, T.-S. Chou, S. Bin Anooz, A. Fiedler, Z. Galazka, A. Popp, Perspectives on MOVPE-grown (100) β-Ga2O3 thin films and its Al-alloy for power electronics application, Appl. Phys. Lett. 121 (2022) 240503.
[33] T.-S. Chou, S. Bin Anooz, R. Grüneberg, T.T.V. Tran, J. Rehm, Z. Galazka, A. Popp, Homoepitaxial growth rate measurement and surface morphology monitoring of MOVPE-grown Si-doped (100) β-Ga2O3 thin films using in-situ reflectance spectroscopy, J. Cryst. Growth 603 (2023) 127003.
[34] D.E. Aspnes, Local-field effects and effective-medium thoery: A microscopic perspective, Am. J. Phys 50 (1982) 704–709, https://doi.org/10.1119/1.12734.
[35] M. Born, E. Wolf, Principles of optics: electromagnetic theory of propagation, interference and diffraction of light, Elsevier, 2013.
[36] S.J. Byrnes, Multilayer optical calculations, Arxiv. (2016) 1–20. 10.48550/ARXIV.1603.02720.
[37] D. Gogova, M. Ghezellou, D.Q. Tran, S. Richter, A. Papamichail, J.U. Hassan, A. R. Persson, P.O.Å. Persson, O. Kordina, B. Monemar, M. Hilfiker, M. Schubert, P. P. Paskov, V. Darakchieva, Epitaxial growth of β-Ga_2O_3 by hot-wall MOCVD, AIP Adv. 12 (2022) 055022, https://doi.org/10.1063/5.0087571.
[38] S. Nakagomi, Y. Kokubun, Crystal orientation of β-Ga_2O_3 thin films formed on c-plane and a-plane sapphire substrate, J. Cryst. Growth 349 (2012) 12–18, https://doi.org/10.1016/j.jcrysgro.2012.04.006.
[39] S. Rafique, L. Han, A.T. Neal, S. Mou, M.J. Tadjer, R.H. French, H. Zhao, Heteroepitaxy of N-type β-Ga_2O_3 thin films on sapphire substrate by low pressure chemical vapor deposition, Appl. Phys. Lett. 109 (2016) 132103, https://doi.org/10.1063/1.4963820.
[40] I.H. Malitson, F.V. Murphy, W.S. Rodney, Refractive Index of Synthetic Sapphire, J. Opt. Soc. Am. 48 (1958) 72–73, https://doi.org/10.1364/JOSA.48.000072.
[41] I. Bhaumik, R. Bhatt, S. Ganesamoorthy, A. Saxena, A.K. Karnal, P.K. Gupta, A. K. Sinha, S.K. Deb, Temperature-dependent index of refraction of monoclinic Ga_2O_3 single crystal, Appl. Opt. 50 (2011) 6006–6010, https://doi.org/10.1364/AO.50.006006.
[42] Z. Cheng, M. Hanke, Z. Galazka, A. Trampert, Thermal expansion of single-crystalline β-Ga_2O_3 from RT to 1200 K studied by synchrotron-based high resolution x-ray diffraction, Appl. Phys. Lett. 113 (2018) 182102, https://doi.org/10.1063/1.5054265.
[43] H.E. Bennett, J.O. Porteus, Relation Between Surface Roughness and Specular Reflectance at Normal Incidence, J. Opt. Soc. Am. 51 (1961) 123, https://doi.org/10.1364/josa.51.000123.
[44] D.A.G. Von, Bruggeman, Berechnung verschiedener physikalischer Konstanten von heterogenen Substanzen, Ann. Phys. 5 (1935) 636–664.
[45] T. Onuma, S. Saito, K. Sasaki, T. Masui, T. Yamaguchi, T. Honda, A. Kuramata, M. Higashiwaki, Spectroscopic ellipsometry studies on β-Ga_2O_3 films and single crystal, Jpn. J. Appl. Phys. 55 (2016) 1202B2, https://doi.org/10.7567/JJAP.55.1202B2.
[46] M. Rebien, W. Henrion, M. Hong, J.P. Mannaerts, M. Fleischer, Optical properties of gallium oxide thin films, Appl. Phys. Lett. 81 (2002) 250–252, https://doi.org/10.1063/1.1491613.
[47] M. Rössle, C.N. Wang, P. Marsik, M. Yazdi-Rizi, K.W. Kim, A. Dubroka, I. Marozau, C.W. Schneider, J. Humlíček, D. Baeriswyl, C. Bernhard, Optical probe of ferroelectric order in bulk and thin-film perovskite titanates, Phys. Rev. B - Condens. Matter Mater. Phys. 88 (2013) 104110, https://doi.org/10.1103/PhysRevB.88.104110.
[48] D. Carrasco, E. Nieto-Pinero, M. Alonso-Orts, R. Serna, J.M.S. Juan, M.L. Nó, J. Jesenovec, J.S. McCloy, E. Nogales, B. Méndez, Temperature-dependent anisotropic refractive index in β-Ga2O3: application in interferometric thermometers, Nanomaterials 13 (2023) 1126.
[49] M.E. Thomas, S.K. Andersson, R.M. Sova, R.I. Joseph, Frequency and temperature dependence of the refractive index of sapphire, Infrared Phys. Technol. 39 (1998) 235–249, https://doi.org/10.1016/S1350-4495(98)00010-3.
[50] C.K. Carniglia, D.G. Jensen, Single-layer model for surface roughness, Appl. Opt. 41 (2002) 3167, https://doi.org/10.1364/ao.41.003167.
[51] H. Fujiwara, Spectroscopic Ellipsometry: Principles and Applications, 6th ed., John Wiley & Sons, 2007. 10.1002/9780470060193.
[52] A.D. Berdie, S. Jitian, Ellipsometric determination of the thickness and the refractive index of superficial films deposited on metal mirrors, J. Phys. Conf. Ser. 1426 (2020) 012017, https://doi.org/10.1088/1742-6596/1426/1/012027.
[53] F. Orlandi, F. Mezzadri, G. Calestani, F. Boschi, R. Fornari, Thermal expansion coefficients of β-Ga_2O_3 single crystals, Appl. Phys Express 8 (2015) 111101, https://doi.org/10.7567/APEX.8.111101.